*M. ABDALLAH, A. S. FOUDA**
S. M. EL-ASHREY

Scientific paper
UDC:620.193.197.6:669.14.018.8=20

Corrosion inhibiting properties of some crown ethers on corrosion of stainless steel (types 304 and 316) in hydrochloric acid

Crown ethers as macrocyclic compounds constitute a potential class of corrosion inhibitors. The effect of some types of crown ethers on the corrosion behavior of stainless steels of types 304 and 316 in 2M HCl at different temperatures was investigated. Loss in mass and galvanostatic polarization techniques were used to achieve this purpose. In addition surface examinations and morphological studies were applied using scanning electron microscope (SEM) and emission dispersive X-ray analysis (EDX) to study the nature of the protective film formed in absence and presence of these compounds. The inhibition efficiency of these compounds was found to increase with concentration and decrease with rising temperature. The adsorption of these compounds was found to obey Temkin's adsorption isotherms. The values of activation energy and free energy of adsorption indicated physical adsorption of these compounds on the surface. Galvanostatic polarization studies showed that crown ethers act as mixed type inhibitors and retard the dissolution of stainless steels. All the results achieved were compared and discussed and the investigated crown ethers were arranged depending on their effectiveness as corrosion inhibitors of types 304SS and 316SS.

***Keywords**: stainless steel, 304SS, 316SS, crown ethers, corrosion inhibitors.*

1. INTRODUCTION

The austenitic stainless steel contains Fe, Cr, Ni and/or Mo. Chromium is ferrite stabilizer. On increasing the Cr content of the alloy increases the corrosion rate,[1] in H_2SO_4, but, the corrosion resistance is increased in the presence of Ni and Mo alloying metals. Ni and Mo additions increase the corrosion resistance of the alloy in HCl and H_3PO_4 environments [2]. Si and Cr exhibit active-passive behavior in sodium or potassium hydroxide solutions [3].

Organic substances used as corrosion inhibitors are at the moment selected essentially from empirical knowledge based on their macroscopical physicochemical properties. Relatively few efforts have been directed towards the theoretical prediction of the efficiency of corrosion inhibitors. Many of organic inhibitors usually promote the formation of chelates at the surface, which prevent corrosion [4]. Under these conditions, for a given metal, the efficiency of the inhibitor depends on the stability of the formed chelate. The inhibitor molecule should have centers capable of forming bonds with the metal surface by electron transfer. Thus, the metal acts as an electrophile, whereas the inhibitor acts as Lewis base, whose nucleophilic centers are normally hetero atoms, with free electronic pairs which are readily available for sharing. The most common organic substances with these characteristics are those containing O, N and / or S atoms.

There are many different uses of crown ethers in analytical chemistry, biological activity and phase transfer catalyst, [5-7] but there are little work to use the crown ether as corrosion inhibitors. The aim of this work is to study the effect of some selected crown ethers (DB18C6, K-22DD, K-222 & DB24C8) on the corrosion rate of two types of austenitic stainless steels (304SS & 316SS) in 2M HCl solution at different temperatures using different independent techniques (loss in mass, galvanostatic polarization, scanning electron microscope (SEM) and emission dispersive x-ray analysis (EDX).

2. EXPERIMENTAL TECHNIQUES

The type 304SS has the chemical composition in wt%: 0.08 C, 2.0 Mn, 0.045 P, 0.03 S 1.0 Si, 18.0 Cr, 8.0 Ni and the remainder is Fe where the type 316SS has 0.08 C, 2.0 Mn, 0.045 P, 0.03 S 1.0 Si,17.0 Cr, 12.0 Ni, 2.5 Mo and the remainder is

Address authors: Chem. Dep. Faculty of science, Benha University, Benha, Egypt, E-mail: metwally552 @hotmail.com. *Chem. Dep. Faculty of science, Mansoura University, Mansoura, Egypt. E-mail: asfouda @ yahoo.com

Fe. For loss in mass measurements, stainless steel specimens used in the form of sheets having surface area of 4.0 cm^2. Loss in mass measurements was carried out as described elsewhere [8]. Galvanostatic polarization studies were carried out using EG & G model 173 potentiostat / galvanostat. Three types of electrodes were used (working electrodes, saturated calomel reference electrode (SCE) and foil auxiliary electrode. Before each experiment, the working electrode was polished with different grade emery papers, degreased with acetone, rinsed by distilled water and finely dried. Scanning electron microscope (SEM) of the type (XL30) and emission dispersive X-ray (EDX) of model EDAX were used in parallel in this work. All micrographs of the corroded specimens were taken at a magnification of (x500). The chemical structure of the investigated crown ethers are:

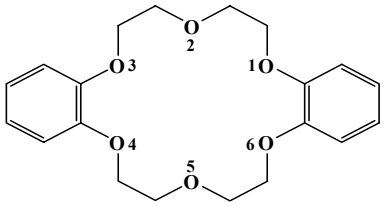

6,7,9,10,17,18,20,21-Octahydro-5,8,11,16,19,22-hexaoxa-dibenzo[a,j]cyclooctadecene
Dibenzo-18 crown-6 (DB18C8)

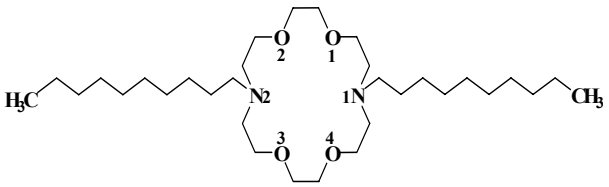

4,13-Diacetyl, 1, 7, 10, 16-tetraoxa-4, 13-diazacyclo-octadecan - Kryptofix 22DD (Kry-22DD)

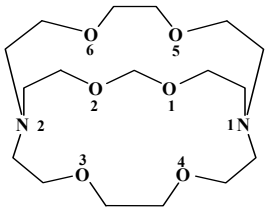

4,7,13,16,21,23-Hexaoxa-1,10-diaza-bicyclo[8.8.7] pentacosane - Kryptofix 222(Kry-222)

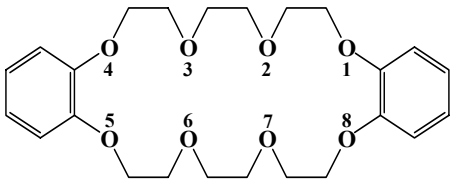

4, 7, 13, 16, 21, 24-hexa-oxa-1, 10-diazo-bicyclo-(8,8,8)-hexacosane - Dibenzo-24 crown-8 (DB24C8)

3. RESULTS AND DISCUSSION

3.1. Loss in mass measurements

The effect of four types of crown ethers on the loss in mass values of stainless steel of types 304SS and 316SS in 2M HCl solution was investigated. This can be quantified by using the simple relationship: [9]

$$\text{loss in mass}\ (\text{mg.cm}^{-2}) = \frac{M_B - M_A}{A} \quad (1)$$

where, M_A and M_B are the mass of metal after and before exposure to the corrosive solution (mg.) and A is the exposed surface area (cm^2).

Figs. (1) represents, the mass loss-time curves of types 304SS in 2M HCl in absence and presence of different concentrations of DB18C6 at 303K. It is seen from this figure, by increasing the concentration of this compound, the loss in mass values were decreased. By the same way we obtained the same behavior in case of the other investigated crown ethers and also in case of 316SS type. This means that the presence of crown ethers retards the corrosion of stainless steels. In other words, these compounds act as corrosion inhibitors. The linear variations of mass loss values with time in most cases of inhibited stainless steels (304SS and 316SS) indicated the absence of insoluble surface films during corrosion [10]. In absence of surface films, the inhibitors are first adsorbed on the metal surface and thereafter impede corrosion either by merely blocking the reaction sites (anodic and cathodic) or by altering the mechanism of the anodic and cathodic partial processes.

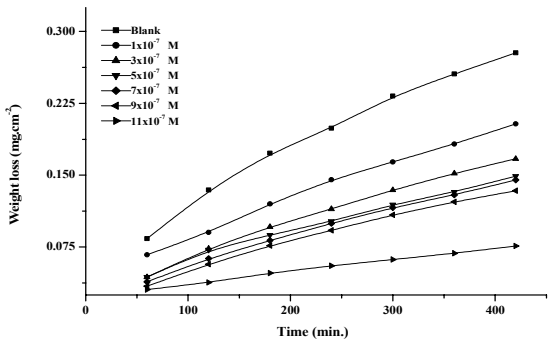

Fig. (1): Mass loss-time curves of 304SS in 2M HCl in absence and presence of different concentrations of DB18C6 at 303K.

A comparative study on the dissolution process of 304SS and 316SS types in absence and presence of the above mentioned crown ethers reflects some interesting features:

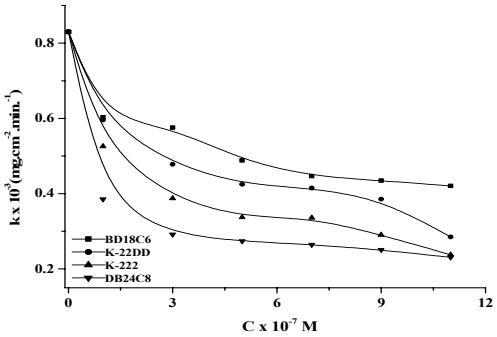

Fig. (2): Effect of crown ethers concentration on the corrosion rate (k) of 304 stainless steel.

1) Increasing the concentration of crown ethers (from $1x10^{-7}$ M to $1.1x10^{-6}$ M) remarkably decreeses the rate of corrosion of 304SS and 316SS types, Fig. (2). The effectiveness of crown ethers as corrosion inhibitors for the two types of stainless steel varies according to the following order:

DB18C6 < K-22DD < K-222 < DB24C8

2) The loss in mass values of 316SS in absence and presence of crown ethers are less than the corresponding values in case of 304SS type, Fig.(3)

To clear up the effect of crown ethers on the inhibition mechanism of different types of stainless steel, the degree of surface coverage (θ) the percentage inhibition efficiency (%IE) values were calculated from these equations [11]:

$$\theta = 1 - \frac{M_{add}}{M_{free}} \qquad (2)$$

$$\% IE = \frac{M_{free} - M_{add}}{M_{free}} x100 \qquad (3)$$

where, M_{free} and M_{add} are loss in mass values in the corrosive medium, and in the inhibited medium at given time values and temperature, each of them are in ($mg.cm^{-2}$) respectively.

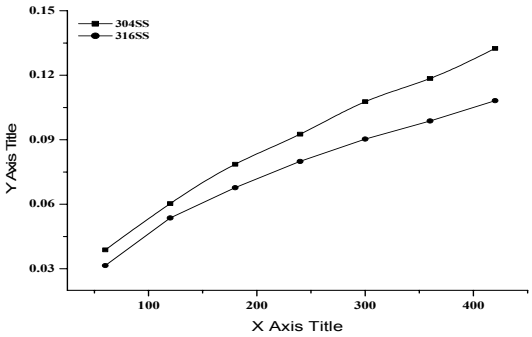

Fig. (3): Mass loss-time curves of 304SS type in presence of $1x10^{-7}$ M of different types of crown ethers.

Table (1): percentage inhibition efficiency values (%IE) of 304SS and 316SS types in presence of different concentrations of crown ethers at 303K.

concentration (M)	304SS				316SS			
	DB18C6	K-22DD	K-222	DB24C8	DB18C6	K-22DD	K-222	DB24C8
$1x10^{-7}$	27.0	28.1	36.6	53.5	14.8	23.7	21.4	37.2
$3x10^{-7}$	42.4	53.3	41.1	64.8	23.4	35.3	25.0	45.5
$5x10^{-7}$	48.8	59.3	42.6	67.0	25.1	39.7	26.0	49.3
$7x10^{-7}$	50.0	59.5	46.4	68.1	29.1	40.1	26.6	53.8
$9x10^{-7}$	53.5	65.0	47.6	69.8	33.2	47.0	26.9	56.0
$1.1x10^{-6}$	72.0	65.6	49.3	71.4	58.7	51.0	26.9	56.8

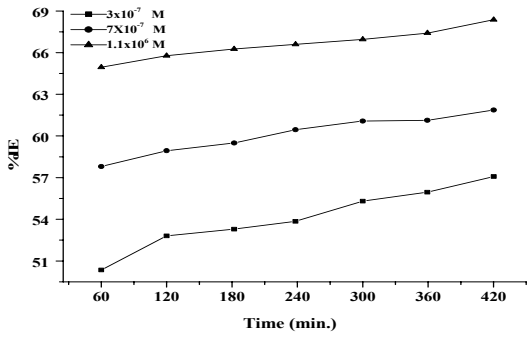

Fig. (4): Relation between the percentage inhibition values (%IE) with the immersion time for 316SS in 2M HCl in presence of different concentrations of DB24C8 at 303K.

Table (1), represents the variation of %IE values of 304SS and 316SS types in presence of different concentrations of crown ethers at 303K. The %IE values increase by increasing the concentration of different types of crown ethers and also by increasing the immersion time, Fig. (4), due to the formation of a barrier film from crown ether molecules which prevents the attack of acid on the metal surface. Attempts were made to fit (θ) values to different adsorption isotherms. The best fit was obtained with Temkin's adsorption isotherm according to the following equation:

$$ln\ K\ C = a\ \theta \qquad (4)$$

where, θ is the degree of surface coverage, a is the molecule interaction parameter, C is the inhibitor concentration in the bulk solution and K is the equilibrium constant of the adsorption reaction which related to the standard free energy of adsorption ($\Delta G°_{ads.}$) by this equation:

$$K = \frac{1}{55.5} \exp\left[\frac{-\Delta G^{o}_{ads}}{RT} \right] \qquad (5)$$

where, R is the universal gas constant and T is the absolute temperature.

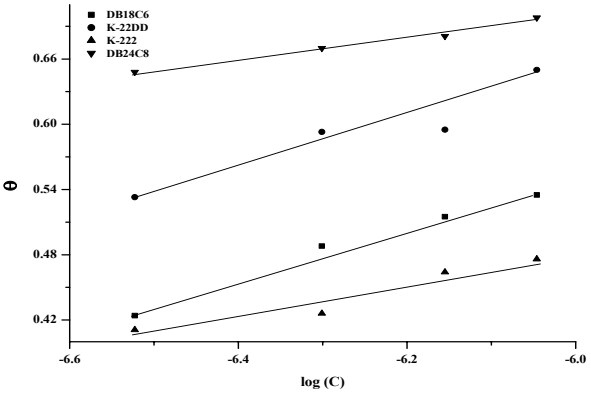

Fig. (5): Curve fitting of corrosion data for stainless steel of type 304 in 2M HCl in presence of different concentrations of crown ethers to the Temkin's adsorption isotherm at 303K.

The relation between θ and log C gives straight lines, Fig. (5). This means, the adsorption of crown ethers obeys Temkin's adsorption isotherm. This suggests the used crown ethers block the reaction sites on the surface of stainless steels by adsorption [12], and reduces the available area for further corrosion reaction. Also, the kinetic-thermodynamic model of El Awady et. al. [13] is valid to operate the present adsorption data according to the following equation:

$$\log \theta / (1-\theta) = \log K' + y \log C \qquad (6)$$

The equilibrium constant of adsorption $K=K'^{(1/y)}$, where 1/y is the number of the surface active sites occupied by only one crown ether molecule and (C) is the bulk concentration of the inhibitor. The calculated values of 1/y, K and $\Delta G°_{ads.}$ are given in Table (2). Inspection of the data shows that the values of ($\Delta G°_{ads.}$) and its negative sign indicated the adsorption of crown ethers on the surface of the two types of stainless steel is proceeding spontaneously and is accompanied by a highly-efficient adsorption. It is worth noting that the value of 1/y is less than unity. This means the given inhibitor molecules will not occupy more than one active site. In general, the values of ($\Delta G°_{ads.}$) obtained from El-Awady model are very close to the values obtained from Temkin's adsorption isotherms.

Table (2): The molecule interaction parameter (a), the equilibrium constant of adsorption reaction (K), free energy of binding (ΔG^{o}_{ads}) and number of surface active sites (1/y) for crown ethers at 303K.*

Stainless steel type	inhibitor	Temkin			Kinetic model		
		a	K	$-\Delta G^{o}_{ads}$ KJ mol^{-1}	1/y	K	$-\Delta G^{o}_{ads}$ KJ mol^{-1}
304SS	DB18C6	0.830	1348	10.87	0.238	1440	11.03
	K-22DD	0.822	1399	10.85	0.239	1325	10.82
	K-222	1.913	1260	10.69	0.796	1484	11.11
	DB24C8	1.353	1250	10.67	0.447	1373	10.91
316SS	DB18C6	0.949	1540	11.20	0.257	1491	11.12
	K-22DD	0.887	1480	11.10	0.359	1476	11.09
	K-222	5.860	2211	12.11	0.305	2417	12.34
	DB24C8	1.023	1439	11.03	0.452	1439	11.03

The effect of temperature on the dissolution process was studied. It was found that the weight loss values increase at all concentrations with rising the temperature from 303K to 333K. This is attributed to the desorption of some crown ether molecules from the surface at higher temperatures suggesting of physical adsorption type. The thermodynamic activation parameters were calculated and discussed. The values of corrosion rate (k) which obtained at the above mentioned temperatures permit the calculation of the Arrhenius activation energy (E_a^*) according to the following equation [14]:

$$\log k = \frac{-E_a^*}{RT} + A \qquad (7)$$

where, (A) is a constant depends on the metal type and the electrolyte. The form of Arrhenius equation is applicable in the present study Fig. (6).The values of E_a^* were calculated from the slopes of the straight lines. From Table (3), the values of E_a^* were increased by increasing the concentration of crown ethers indicating the dissolution under these conditions is activation controlled. This indicates the energy barrier of the corrosion reaction increases in the presence of these additives.

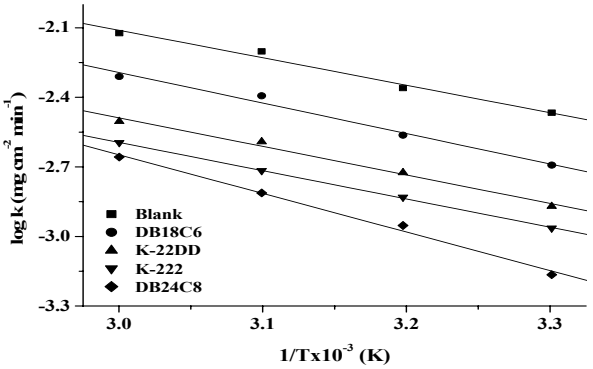

Fig. (6): log. corrosion rate vs. 1/T of 304SS in 2M HCl in absence and presence of 1x10^{-7} M of different types of crown ethers

Table (3): Activation energy values (E_a^* in KJ mol^{-1}) of the dissolution of 304SS and 316SS in 2M HCl in absence and presence of different concentrations of crown ethers.

inhibitor	304SS			316SS		
	1x10^{-7} M	5x10^{-7} M	9x10^{-7} M	1x10^{-7} M	5x10^{-7} M	9x10^{-7} M
Blank	---	28.97	---	---	50.12	---
DB18C6	37.96	40.4	43.49	52.83	54.23	56.81
K-22DD	48.01	48.18	51.62	54.33	55.7	58.39
K-222	49.2	51.25	55.77	56.21	57.99	59.69
DB24C8	51.02	54.56	57.66	56.68	61.23	61.67

Also, free energies of activation (ΔG^*) were calculated by applying the transition state equation [15]:

$$\Delta G^* = RT\left[\ln\frac{kT}{h} - \ln(\text{rate})\right] \qquad (8)$$

where: h is Plank's constant, k is Boltzman's constant, R is gas constant and T is the absolute temperature

Moreover, The enthalpy (ΔH^*) and the entropy (ΔS^*) of activation values were calculated by applying the following equations:

$$\Delta H^* = E_a^* - RT \qquad (9)$$

$$\Delta S^* = \frac{\Delta H^* - \Delta G^*}{T} \qquad (10)$$

The values of the thermodynamic parameter for the dissolution of 304SS and 316SS types listed in Tables (4-6). Inspection of these data reveals that the values of ΔH^* and ΔG^* in presence of crown ethers increase over that the uninhibited solution. This implies the energy barrier of the corrosion reaction in presence of crown ethers increases. On the other hand, ΔS^* values are lower and have negative values in presence of crown ethers. This means, addition of these compounds causes a decrease in the disordering in going from reactants to the activated complexes [16]. Also, it is evident that the values of ΔG^* increase with rising temperature where the constantly values of ΔH^* indicated that the mechanism of the corrosion reaction was not changed by raising the temperatures. On the other hand, the low values of ΔH^* suggested, the crown ethers are physically adsorbed on the surface of stainless steels [17].

Table (4): Thermodynamic activation parameters (ΔG^*, ΔH^* in KJ mol^{-1} & ΔS^* in J mol^{-1}) of 304SS and 316SS dissolution in 2M HCl at different temperatures.

Temperature (K	304SS			316SS		
	ΔG^*	ΔH^*	$-\Delta S^*$	ΔG^*	ΔH^*	$-\Delta S^*$
303	84.94	26.45	193.0	86.23	47.60	127.5
313	87.44	26.37	195.1	88.44	47.52	130.7
323	90.15	26.29	197.7	90.57	47.44	133.5
333	92.7	26.20	199.7	93.49	47.35	138.5

Table (5): Thermodynamic activation parameters (ΔG^*, ΔH^* in KJ mol^{-1} & ΔS^* in J mol^{-1}) of 304SS dissolution in 2M HCl in presence of different concentrations of crown ethers at different temperatures.

(I) DB18C6									
Temperature (K)	$1x10^{-7}$ M			$5x10^{-7}$ M			$9x10^{-7}$ M		
	ΔG^*	ΔH^*	$\tilde{}\Delta S^*$	ΔG^*	ΔH^*	$\tilde{}\Delta S^*$	ΔG^*	ΔH^*	$\tilde{}\Delta S^*$
303	85.51	35.44	165.3	85.95	37.88	158.6	86.37	40.97	149.8
313	88.04	35.36	168.3	88.39	37.80	161.6	88.79	40.89	153.1
323	90.53	35.28	171.1	90.95	37.72	164.8	91.58	40.81	157.2
333	93.02	35.19	173.7	93.36	37.63	167.4	93.64	40.72	158.9
(II) K-22DD									
Temperature (K)	$1x10^{-7}$ M			$5x10^{-7}$ M			$9x10^{-7}$ M		
	ΔG^*	ΔH^*	$\tilde{}\Delta S^*$	ΔG^*	ΔH^*	$\tilde{}\Delta S^*$	ΔG^*	ΔH^*	$\tilde{}\Delta S^*$
303	85.88	45.49	133.3	86.56	45.66	135.0	87.25	49.10	125.9
313	88.49	45.41	137.6	89.16	45.58	139.2	89.65	49.02	129.8
323	90.72	45.33	140.5	91.62	45.50	142.8	92.15	48.94	133.8
333	93.14	45.24	143.8	93.76	45.41	145.2	94.35	48.85	136.6
(III) K-222									
Temperature (K)	$1x10^{-7}$ M			$5x10^{-7}$ M			$9x10^{-7}$ M		
	ΔG^*	ΔH^*	$\tilde{}\Delta S^*$	ΔG^*	ΔH^*	$\tilde{}\Delta S^*$	ΔG^*	ΔH^*	$\tilde{}\Delta S^*$
303	86.12	46.68	130.2	87.01	48.73	126.3	87.59	53.25	113.3
313	88.93	46.60	135.2	89.50	48.65	130.5	89.97	53.17	117.6
323	91.09	46.52	138.0	91.96	48.57	134.3	92.29	53.09	121.4
333	93.35	46.43	140.9	94.08	48.48	136.9	94.62	53.00	125.0
(IV) DB24C8									
Temperature (K)	$1x10^{-7}$ M			$5x10^{-7}$ M			$9x10^{-7}$ M		
	ΔG^*	ΔH^*	$\tilde{}\Delta S^*$	ΔG^*	ΔH^*	$\tilde{}\Delta S^*$	ΔG^*	ΔH^*	$\tilde{}\Delta S^*$
303	86.28	48.50	124.7	87.37	52.04	116.6	87.92	55.14	108.2
313	89.16	48.42	130.2	89.93	51.96	121.3	90.39	55.06	112.9
323	91.22	48.34	132.8	92.32	51.88	125.2	92.78	54.98	117.1
333	93.48	48.25	135.8	94.84	51.79	129.3	94.84	54.89	120.0

Table (6): Thermodynamic activation parameters (ΔG^*, ΔH^* in KJ mol^{-1} & ΔS^* in J mol^{-1}) of 316SS dissolution in 2M HCl in presence of different concentrations of crown ethers at different temperatures

(I) DB18C6									
Temperature (K)	1x10^{-7} M			5x10^{-7} M			9x10^{-7} M		
	ΔG^*	ΔH^*	$-\Delta S^*$	ΔG^*	ΔH^*	$-\Delta S^*$	ΔG^*	ΔH^*	$-\Delta S^*$
303	86.62	50.31	119.8	86.71	51.71	115.5	86.76	54.29	107.2
313	88.99	50.23	123.8	89.37	51.63	120.6	89.33	54.21	112.2
323	91.07	50.15	126.7	91.57	51.55	123.9	91.60	54.13	116.0
333	93.80	50.06	131.3	93.81	51.46	127.2	93.72	54.04	119.2
(II) Kry-22DD									
Temperature (K)	1x10^{-7} M			5x10^{-7} M			9x10^{-7} M		
	ΔG^*	ΔH^*	$-\Delta S^*$	ΔG^*	ΔH^*	$-\Delta S^*$	ΔG^*	ΔH^*	$-\Delta S^*$
303	86.97	51.81	116.0	87.10	53.18	111.9	87.22	55.87	103.5
313	89.38	51.73	120.3	89.81	53.10	117.3	89.89	55.79	108.9
323	91.67	51.65	123.9	92.03	53.02	120.8	92.09	55.71	112.6
333	94.01	51.56	127.5	94.13	52.93	123.7	94.15	55.62	115.7
(III) Kry-222									
Temperature (K)	1x10^{-7} M			5x10^{-7} M			9x10^{-7} M		
	ΔG^*	ΔH^*	$-\Delta S^*$	ΔG^*	ΔH^*	$-\Delta S^*$	ΔG^*	ΔH^*	$-\Delta S^*$
303	87.31	53.69	111.0	87.57	55.47	105.9	87.76	57.17	101.0
313	89.63	53.61	115.1	90.33	55.39	111.7	90.53	57.09	106.9
323	92.07	53.53	119.3	92.56	55.31	115.3	92.71	57.01	110.5
333	94.24	53.44	122.5	94.52	55.22	118.0	94.65	56.92	113.3
(IV) DB24C8									
Temperature (K)	1x10^{-7} M			5x10^{-7} M			9x10^{-7} M		
	ΔG^*	ΔH^*	$-\Delta S^*$	ΔG^*	ΔH^*	$-\Delta S^*$	ΔG^*	ΔH^*	$-\Delta S^*$
303	87.66	54.16	110.5	87.97	58.71	96.6	88.27	59.15	96.10
313	90.10	54.08	115.1	90.68	58.63	102.4	91.03	59.07	102.1
323	92.51	54.00	119.2	92.80	58.55	106.0	93.19	58.99	105.9
333	94.58	53.91	122.1	94.85	58.46	109.3	95.10	58.90	108.7

3.2. Galvanostatic polarization measurements

Figures (7) represents the galvanostatic polarization curves (Tafel plots) of the type 304SS in 2M HCl in absence and presence of different concentrations of K-222 at 303K. The intercept of anodic and cathodic Tafel lines provides the corrosion current $I_{corr.}$ and their slopes give anodic β_a and cathodic β_c Tafel constants. Also, The values of θ and %IE are given from the following equations: [9]

$$\theta = 1 - \frac{I_{inh.}}{I_{free}} \qquad (11)$$

$$\%IE = \left(1 - \frac{I_{inh.}}{I_{free}}\right) x\, 100 \qquad (12)$$

where, $I_{inh.}$ and I_{free} are the corrosion current densities in presence and absence of crown ethers, respectively.

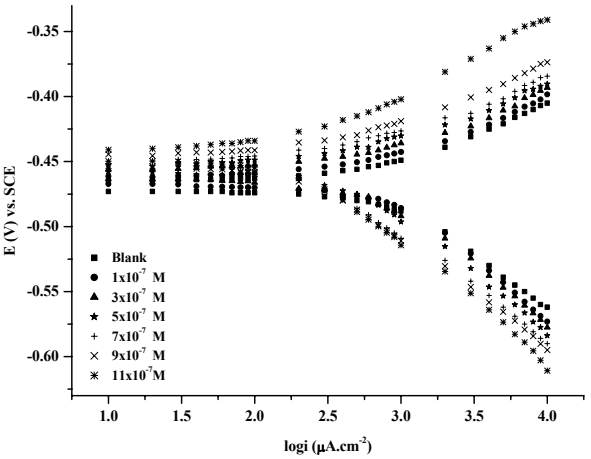

Fig. (7): Galvanostatic polarization curves of 304SS in 2MHCl in absence and presence of different concentrations of K-222 at 303K.

Table (7): Effect of crown ethers on the corrosion potential (E_{corr}), corrosion current density ($I_{corr.}$), Tafel slopes (β_a & β_c), degree of surface coverage (θ) and percentage inhibition efficiency (%IE) of 304SS in 2M HCl at 303K.

concentration (M)	$-E_{corr}$ (mV)	$I_{corr.}$ ($\mu A\ cm^{-2}$)	β_a ($mVdec^{-1}$)	β_c ($mVdec^{-1}$)	θ	%IE
Blank						
2M HCl	462	731	49	89	---	---
DB18C6						
$1x10^{-7}$	458	581	45	86	0.21	20.5
$3x10^{-7}$	454	568	45	91	0.22	22.3
$5x10^{-7}$	451	421	45	87	0.42	42.4
$7x10^{-7}$	443	356	44	91	0.51	51.3
$9x10^{-7}$	441	318	44	93	0.57	56.5
$1.1x10^{-6}$	436	303	45	97	0.59	58.6
K-22DD						
$1x10^{-7}$	460	556	45	84	0.24	23.9
$3x10^{-7}$	454	523	45	95	0.29	28.4
$5x10^{-7}$	452	436	44	95	0.40	40.4
$7x10^{-7}$	448	401	41	97	0.45	45.1
$9x10^{-7}$	445	333	39	98	0.54	54.4
$1.1x10^{-6}$	439	322	38	105	0.56	55.9
K-222						
$1x10^{-7}$	456	581	43	93	0.21	20.5
$3x10^{-7}$	455	483	44	91	0.34	34.6
$5x10^{-7}$	453	375	45	88	0.49	48.7
$7x10^{-7}$	453	323	45	90	0.56	55.8
$9x10^{-7}$	451	295	48	93	0.60	59.6
$1.1x10^{-6}$	447	172	61	88	0.76	76.4
DB24C8						
$1x10^{-7}$	462	330	40	82	0.55	54.8
$3x10^{-7}$	461	257	47	88	0.65	64.8
$5x10^{-7}$	459	206	48	87	0.72	71.9
$7x10^{-7}$	451	195	47	100	0.73	73.3
$9x10^{-7}$	447	143	44	100	0.81	80.5
$1.1x10^{-6}$	444	133	45	109	0.82	81.8

Table (8): Effect of crown ethers on the corrosion potential (E_{corr}), corrosion current density ($I_{corr.}$), Tafel slopes (β_a & β_c), degree of surface coverage (θ) and percentage inhibition efficiency (%IE) of 316SS in 2M HCl at 303K.

concentration (M)	$-E_{corr}$ (mV)	$I_{corr.}$ ($\mu A\ cm^{-2}$)	β_a ($mVdec^{-1}$)	β_c ($mVdec^{-1}$)	θ	%IE
Blank						
2M HCl	462	731	49	89	---	---
DB18C6						
$1x10^{-7}$	445	439	88	97	0.21	20.5
$3x10^{-7}$	444	398	85	94	0.28	27.9
$5x10^{-7}$	429	347	72	103	0.37	37.1
$7x10^{-7}$	428	338	71	104	0.39	38.8
$9x10^{-7}$	428	317	74	101	0.43	42.6
$1.1x10^{-6}$	422	194	61	92	0.65	64.9

K-22DD						
$1x10^{-7}$	424	242	67	95	0.56	56.2
$3x10^{-7}$	394	155	51	102	0.72	71.9
$5x10^{-7}$	393	123	51	100	0.78	77.7
$7x10^{-7}$	390	119	50	101	0.79	78.5
$9x10^{-7}$	387	103	50	100	0.81	81.4
$1.1x10^{-6}$	367	100	44	113	0.82	81.9
K-222						
$1x10^{-7}$	428	111	62	83	0.80	79.9
$3x10^{-7}$	422	93	58	86	0.83	83.2
$5x10^{-7}$	419	69	54	91	0.88	87.5
$7x10^{-7}$	417	58	52	92	0.89	89.4
$9x10^{-7}$	414	46	50	94	0.92	91.6
$1.1x10^{-6}$	440	38	60	82	0.93	93.2
DB24C8						
$1x10^{-7}$	425	114	61	87	0.79	79.4
$3x10^{-7}$	422	94	58	89	0.83	82.9
$5x10^{-7}$	421	77	58	86	0.86	86.1
$7x10^{-7}$	407	74	51	93	0.87	86.5
$9x10^{-7}$	407	59	49	89	0.89	89.3
$1.1x10^{-6}$	407	57	50	93	0.90	89.8

The numerical values of the variation of $I_{corr.}$, E_{corr}, β_a, β_c, θ and %IE of the types 304SS and 316SS in 2M HCl at 303K in absence and presence of different concentrations of crown ethers can be depicted from Tables (7-8). Wholly, all the results achieved in Tables (7-8) are permitted to conclude that:

1) Galvanostatic anodic and cathodic polarization curves for the two types of stainless steel exhibit Tafel behavior. Addition of crown ethers caused a shift in both cathodic and anodic polarization curves towards the lower current density region.
2) Both the cathodic and anodic overvoltages were increased by increasing the concentration of crown ethers, and parallel displacement to the more negative and positive values were obtainned, respectively. Thus Tafel plots suggested that the crown ethers enhance both anodic and cathodic reactions and are mixed type inhibittors, but the cathode is more polarized when the external current was applied.
3) The values of $I_{corr.}$ decrease with increasing the concentration of crown ethers, while $E_{corr.}$ Values shift in positive direction. This indicated that the presence of these compounds retards the dissolution of the investigated stainless steels.
4) The Tafel slope values do not change signifycantly in acidic solutions in presence of these compounds, suggesting that these compounds inhibit the corrosion of stainless steels by blocking the active surface sites.
5) The values of θ and %IE increase by increasing the concentration of crown ethers. The effecttiveness of crown ethers as corrosion inhibitors obeyed this sequence:

DB24C8 > K-222 > K-22DD > DB18C6

6) Some small differences are observed between the values of %IE obtained by loss in mass and galvanostatic polarization techniques due to loss in mass measurements give average corrosion rates, while galvanostatic polarization measurements give instantaneous corrosion rate.

3.3. Scanning electron microscopy (SEM)

The morphology of the corroded surface of each specimen was studied using scanning electron microscope. Fig. (8) [from I to V] represents SEM micrographs of 304SS immersed for seven hours in 2M HCl solution in absence and presence of different concentrations of the investigated crown ethers. These micrographs show an extensive etching composed of greenish and dark areas in presence of some white areas. The greenish areas reflect the part of protective film which contains mainly chromium and its oxides, where the white areas represent the ferrite phase and the dark areas represent the pearlite, [mixture of ferrite and cementite (Fe_3C) in a lamellar form].

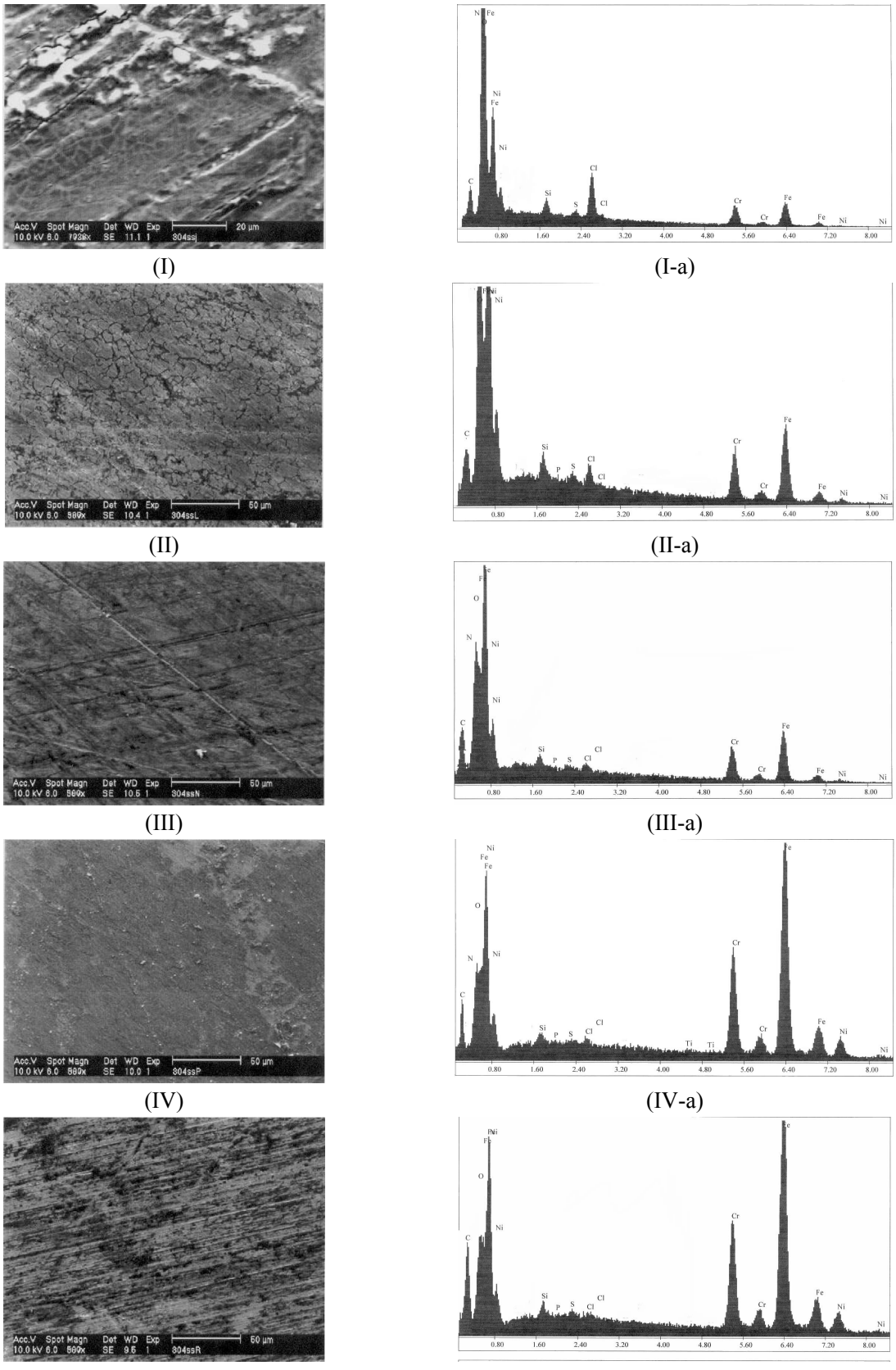

Fig. (8): SEM micrographs (x 500) of 304SS type immersed for 7 hours in 2M HCl in absence of crown ethers (I) in presence of $9x10^{-7}$ M of DB18C6 (II), K-22DD (III), K-222 (IV), DB24C8 (V) and their EDX analysis charts for the same specimens under the same conditions.

For example Fig. (8-II) reveals, the surface was damaged appreciably owing to the corrosion in the presence of $9x10^{-7}$ M of DB18C6 but it is still in better conditions than the specimen exposed to the corrosive medium in absence of inhibitors Fig. (8-I)). Another example is Fig. (8-III), which represents the conditions of 304SS surface in the presence $9x10^{-7}$ M of K-22DD. which provided good protection of the surface. The protective film presented on the surface of 304SS at a concentration of $9x10^{-7}$ M of DB24C8, Fig. (8-V), appears to be very smooth and to cover the whole surface without any flows. This confirms the observed high %IE values of DB24C8 at $9x10^{-7}$ M as it was discussed in loss in mass and galvanostatic polarization results.

3.4. Emission dispersive X-ray analysis (EDX)

Surface analyses of 304SS and 316SS types were carried out using emission dispersive x-ray analysis EDX. The results were plotted on a graph of dN/dE ν. electron energy, as shown in figures (8) [from I-a to V-a] represent the various peaks owing to different elements.

From all analysis charts, it was found that the results of EDX may be explained and discussed depending on the values of weight percentages wt % of carbon and chloride atoms on the surface as follow:

1) In all the charts of EDX the carbon atom peak appears around the value of 0.2 KV and the peak of chloride atom appears at 2.6 KV. As the corrosive medium is 2M HCl solution and the organic additives consist mainly of C, O and/or C, O, N atoms, so the variation of chloride and carbon weight percentages on the surface can be used quantitively to explain the adsorption of crown ethers on the surface of stainless steels.
2) For example, Fig. (8-I-a) represents EDX of 304SS exposed to 2M HCl at 303K for seven hours, where Fig (8-V-a) represents the same sample in the presence of $9x10^{-7}$ M of DB24C8. From comparison the wt % values of carbon were increased from 2.69 % to 4.15 %, on the other hand the wt % values of chloride were decreased in presence of DB24C8 from 2.16 % to 0.31 %. This is due to the replacement of the firstly adsorbed chloride atoms which comes from the corrosive medium by C atoms that comes from crown ethers. These results confirm the adsorption of DB24C8 on the surface of 304SS. wholly, in all cases wt. % values of carbon on the surface were increased by increasing the concentration of the investigated crown ethers. On the other hand, wt % values of chloride were decreased.
3) From Table (9) we may conclude that, the increase in the weight percentage (wt %) of carbon obeys the following sequence:

DB18C6 < K-22DD < K-222 < DB24C8

and vice versa in case of chloride atoms conesquently, the arrangement of crown ethers according to their inhibition efficiencies could be written as follows:

DB18C6 < K-22DD < K-222 < DB24C8

This is also in agreement with the observed order of %IE which given by loss in mass and galvanostatic polarization results.

3.5. Quantum chemical calculations of crown ethers.

The aim of the present part is to investigate the capacity of quantum chemical calculation to predict the efficiencies of crown ethers as corrosion inhibitors. The existence of such a correlation would be of great interest, as it would allow a prior more rational pre-selection of new inhibitors. For this purpose, the structures of the additives have been optimized, and furthermore, the energies and the coefficients of their molecular orbitals have been calculated using ab-initio computer program for this purpose. All the geometric parameters were optimized and the energy being minimized. Table (10), shows the energies and the coefficients of the molecular orbitals of the investigated compounds. The results obtained from the relation between inhibition characteristics and quantum chemical data show that log $i_{corr.}$, mostly depends upon the energies of the highest occupied molecular orbital HOMO. It is evident that, the values of i_{corr} decrease with increasing the energy of the highest occupied molecular orbital (HOMO). By other words, the inhibition efficiency values increase with the ease of ionization of the inhibitor molecule, which means that the inhibitor acts as an electron donor when blocking the corrosion reaction sites [17]. Also, the results in Table (9), show that the energies of HOMO and the ease of ionization of the investigated crown ethers decrease in the order.

DB24C8 > K-222 > K-22DD > DB18C6

Also this agrees with the previously mentioned experimental data.

Table (9): variation of the weight percentage (wt. %) of carbon and chloride obtained from EDX for 304SS and 316SS types in absence and presence of crown ethers.

SS / concn (M)	304SS				316SS			
	wt. % of C		wt. % of Cl		wt. % of C		wt. % of Cl	
	$5x10^{-7}$	$9x10^{-7}$	$5x10^{-7}$	$9x10^{-7}$	$5x10^{-7}$	$9x10^{-7}$	$5x10^{-7}$	$9x10^{-7}$
Blank	2.69	2.69	2.16	2.16	3.75	3.75	0.56	0.56
DB18C6	2.77	2.85	1.94	1.32	3.79	3.85	0.51	0.43
K-22DD	2.84	2.88	0.76	0.68	3.88	3.92	0.48	0.39
K-222	3.11	3.25	0.42	0.39	3.95	3.99	0.33	0.30
DB24C8	3.55	4.15	0.33	0.31	4.24	5.16	0.28	0.25

Table (10): Quantum chemical parameters for different types of crown ethers.

crown ethers	atom	charge denisty	HOMO (EV)	Ionization potential
DB18C6	O (1), O (2) O (3), O (4) O (5), O (6)	-0.192, -0.253 -0.196, -0.210 -0.266, -0.198	-9.404	9.404
K-22DD	N (1), N (2) O (3), O (4) O (5), O (6)	-0.070, -0.053 -0.262, -0.234 -0.244, -0.243	-9.303	9.303
K-222	N (1), N (2) O (1), O (2) O (3), O (4) O (5), O (6)	-0.070, -0.074 -0.277, -0.268 -0.258, -0.253 -0.251, -0.246	-9.176	9.176
DB24C8	O (1), O (2) O (3), O (4) O (5), O (6) O (7), O (8)	-0.188, -0.258 -0.262, -0.184 -0.177, -0.255 -0.251, -0.177	-8.904	8.904

3.6. Inhibition mechanism

The extent of corrosion of 304SS type was found to be higher than that of 316SS type. This is explained on the basis of the variation of the types and percentages of alloying elements. Though, the chromium percentage in case of 304 equal 18% is higher than in case of 316 which equal 17%, it was found that, the corrosion resistevity of the last is higher than that in case of the former. This is mainly due to the increase in the percentage of Ni which equal 12% and the presence of Mo alloying element 2.5% in case of 316SS. In principle, Mo prevents corrosion in three ways. First, it may improve the resistance of the passive film to break down. Second, it may enhance repassivation rates and third, it retards the dissolution process and allows more time for repassivation to repair the film break down sites. The presence of Cr and Mo in the alloys greatly improves their corrosion resistance in acidic chloride solutions [18]. As reported before, Mo was found to inhibit corrosion by forming Mo salt film on the surface of the alloy. This film is difficult to break down. If this film is broken, the surface of the alloy will be enriched with Mo which then further retards the dissolution of the alloy. The above mentioned explanation agrees with several studies which indicated that small addition of Mo as alloying element can improve passivation characteristics [19-27].

Also, the results indicated, the extent of corrosion inhibition of the investigated crown ethers at all concentrations followed the following order:

DB18C6 < K-22DD < K-222 < DB24C8

The above mentioned trend can be explained on the basis of adsorption. These compounds can be adsorbed on the metal surface through the lone pair of electrons of oxygen and/or nitrogen atoms

and delocalized π-electrons of benzene ring. The difference in the inhibition efficiencies can be explained on the basis of the type and the number of hetero atoms in the cavity of these compounds. The cavity of DB18C6 contains six oxygen atoms, K-22DD contains four oxygen and two nitrogen atoms, K-222 contains six oxygen and two nitrogen atoms where BD24C8 contains eight oxygen atoms. The increase in the inhibition efficiency of K-22DD compared with DB18C6 may be attributed to the presence of two nitrogen atoms in the first which have higher availability to donate electrons compared to compound of oxygen atoms and this make the electrostatic interaction with the surface of stainless steel is higher for the former than the last. Also, the presence of the two alkyl branches in K-22DD being electron releasing (+I effect) increase the charge density at the center of adsorption, (i.e.: the two nitrogen atoms), and increase the adsorption of the compounds on the metal surface. On the other hand, although K-222 contains two nitrogen atoms the inhibition efficiency values are less than the corresponding in the case of DB24C8 and this is may be explained on the basis that, the high molecular weight, (448.52) of the later compound compared with the former (376). Also, The presence of the two benzene rings in BD24C8 make the structure very rigid [28], i.e. the structure of DB24C8 due to the presence of benzene rings make the adsorption process achieved in plan compared to the structure of K-222 which adsorbed in two planes through different two cavities. In other words, as the crown ethers contain more than one orienting group (O, N), it can be considered as an ambiodic molecule and its adsorption leads to better corrosion inhibition.

CONCLUSIONS

1) Increasing the concentration of the investigated crown ethers decreases the corrosion of 304SS and 316SS stainless steels. The adsorption of these compounds on the surface of stainless steels obeyed Temkin's adsorption isotherm and the negative values of $\Delta G°_{ads}$ indicated that the adsorption of the investigated crown ethers is proceeding spontaneously.
2) The increase in mass loss values with increasing temperature is suggestive of physical adsorption type and the values of E_a^* revealed, the dissolution of stainless steels is activation controlled. The increase in ΔG^* values with increasing temperature and the constantly values of ΔH^* indicated, the mechanism of the corrosion reaction was not changed by raising the temperatures and the low values of ΔH^* suggested that the crown ethers are physically adsorbed.
3) Addition of crown ethers caused a shift in both cathodic and anodic polarization curves towards the lower current density region suggesting that these compounds are mixed type inhibitors. The decrease in $I_{corr.}$ values with increasing the concentration of crown ethers indicated that these compounds retard the dissolution of stainless steels.
4) The morphology of the corroded surfaces show that the surface of stainless steels in presence of crown ethers are in better conditions than the specimen exposed to the corrosive medium in the absence of inhibitors. Moreover, the EDX results revealed quantitively the replacement of the firstly adsorbed chloride atoms by carbon atoms which come from crown ethers.
5) The inhibition efficiency increases with increasing the energy of HOMO and with the ease of ionization of the molecule, which means that the inhibitor acts as an electron donor when blocking the corrosion reaction sites.

REFERENCES

(1) *J. Marsh*; Advanced organic chemistry; 3rd ed., Wiley eastern, New Delhi, (1988).

(2) *Y. H. Yau and M. A. Streicher;* Corrosion; 47, 352, (1991).

(3) *R. C. Scarberry, D. L. Graver and C. D. Stephens;* Materials protection; 6, 54, ((1967).

(4) *M. Duprat, N. Bui and F. Dabosi;* Corrosion; 35, 392, (1979).

(5) *I. A. Levin*; Inter. Crystalline corrosion and corrosion resistance of metals under stress; Leonard Hill (Books) Ltd., London, (1963).

(6) *H. H. Uhlig*; proceeding of references – Fundamental aspects of stress corrosion cracking – Published by NACE; 86, (1969).

(7) *F. Z. Mylius*; Metallk; 233, (1922).

(8) *P. B. Mouthur and T. V. Vasudeevan*; Corrosion; 38, 17, (1982).

(9) *W. A. Badawy, F. M. El-Kharafi and A. S. El-Azab*; Current Topics in Electrochemistry; 6, 149, (1998).

(10) *M. A. El Hashemy*; M. Sc. Thesis; Chem. Dep., Fuc. of Sci., Mansoura Unv., (2003).

(11) *F. A. Champion*; "Corrosion testing procedures"; second edition, Chapman and Hill, London, (1964).

(12) *A. S. Fouda, M. N. Moussa, F. I. Taha and A. I. Eleanaa*; Corros. Sci.; 26 (9), 719, ((1986).

(13) *Y. A. El-Awady, and A. J. Ahmed*; J. Ind. Chem.; 24A, 601, (1985).

(14) *K. R. Trethewey and John Chamberlain;* Corrosion for Science and Engineering; second edition, Longman Singapore Publishers, (1996), (Singapore).

(15) *F. L. Laque and H. R. Gapson*; Corrosion resistance of metals and alloys; second edition, Reinhold publishing corporation, New York, (1963).

(16) *M. K. Gomma and M. H. Wahdan*; Materials Chemistry and Physics; 39, 209, ((1995).

(17) *J.M. Costa J.M. Lluch;* Corros. Sci.; 24 (11-12), 929, (1984).

(18) *C. P. Dillon;* Mater performance; 31, 51, (1992).

(19) *J. N. Wanklyn;* Corros. Sci.; 21, 211, (1981).

(20) *M. A. A. Tullmin and F. P. A. Robinson;* Corrosion; 44, 664, (1988).

(21) *W. R. Ciesak and D. J. Duquette;* J. Electrochem. Soc.;132, 533 (1985).

(22) *J. R. Galvole, J. B. Lumsden and R. W. Stechle;* J. Electrochem. Soc.; 125, 1204, ((1978).

(23) *K. Sugimoto and Y. Sawada;* Corrosion; 32, 347, (1976).

(24) *M. A. Strechier;* Corrosion; 30, 77, (1974).

(25) *W. Wang, R. Chang and H.Zhua;* Corros. Sci.; 24, 641, (1984).

(26) *R. C. Newman;* Corros. Sci.; 28, 331, (1985).

(27) *K. Asami, K. Hasimoto, T. Masumoto and S. Chimodaria;* Corros. Sci.; 16, 909, (1976).

(28) *S. M. El-Ashrey*; M. Sc. Thesis; Chem. Dep., Fuc. of Sci., Mansoura Unv., (2001).